Pt and PtRu catalyst bilayers increase efficiencies for ethanol oxidation in proton exchange membrane electrolysis and fuel cells

Rakan M. Altarawneh and Peter G. Pickup*

Department of Chemistry, Memorial University, St. John's, Newfoundland, A1B 3X7, Canada

ABSTRACT: Polarization curves, product distributions, and reaction stoichiometries have been measured for the oxidation of ethanol at anodes consisting of Pt and PtRu bilayers and a homogeneous mixture of the two catalysts. These anode structures all show synergies between the two catalysts that can be attributed to the oxidation of acetaldehyde produced at the PtRu catalyst by the Pt catalyst. The use of a PtRu layer over a Pt layer produces the strongest effect, with higher currents than a Pt on PtRu bilayer, mixed layer, or either catalyst alone, except for Pt at high potentials. Reaction stoichiometries (average number of electrons transferred per ethanol molecule) were closer to the values for Pt alone for both of the bilayer configurations but much lower for PtRu and mixed anodes. Although Pt alone would provide the highest overall fuel cell efficiency at low power densities, the PtRu on Pt bilayer would provide higher power densities without a significant loss of efficiency. The origin of the synergy between the Pt and PtRu catalysts was elucidated by separation of the total current into the individual components for generation of carbon dioxide and the acetaldehyde and acetic acid byproducts.

*Corresponding author. Tel.: +1-709-864-8657; Fax: 1-709-864-3702

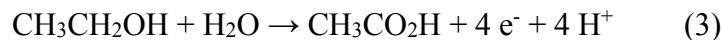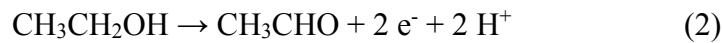*E-mail address: ppickup@mun.ca (P.G. Pickup)*

1. INTRODUCTION

Bio-ethanol is an attractive renewable fuel for use in fuel cells for many reasons, including its high energy density, relative safety, and the well-developed infrastructure for its production and distribution [1, 2]. Direct ethanol fuel cells (DEFC), based on proton-exchange membrane (PEM) technology, are potentially one of the best low emission power sources for transportation [3], and have many other potential applications [2, 4]. Alternatively, ethanol can be oxidized in a PEM ethanol electrolysis cell (EEC) to produce hydrogen for use in fuel cells [5]. Hydrogen fuel cells are already well developed, and can provide much higher power densities than DEFCs [6, 7].

One of the fundamental advantages of fuel cell technology over the use of heat engines is the prospect of higher efficiencies. This will become increasingly important as renewable fuels are substituted for fossil fuels. The overall efficiency of a DEFC (ε_{DEFC}) is determined by the thermodynamic efficiency ($\varepsilon_{rev} = 97\%$ at 25 °C) [8], the potential efficiency ($\varepsilon_E = E_{cell}/E_{rev}$, where E_{cell} is the cell potential and E_{rev} is the reversible cell potential of ca. 1.15 V) [8], the faradaic efficiency (ε_F), and fuel losses due to crossover of ethanol and oxygen through the membrane (ε_C), according to equation 1 [1].

$$\varepsilon_{DEFC} = \varepsilon_{rev}\varepsilon_E\varepsilon_F\varepsilon_C \qquad (1)$$

The faradaic term in eq. 1 arises from the lower number of electrons transferred (n) for the partial oxidation of ethanol to acetaldehyde ($n = 2$; eq. 2) and acetic acid ($n = 4$; eq. 3), relative to complete oxidation to CO_2 ($n = 12$; eq. 4). It is the ratio of the average number of electrons transferred (n_{av}) to the maximum of 12 ($\varepsilon_F = n_{av}/12$).

$$CH_3CH_2OH \rightarrow CH_3CHO + 2\ e^- + 2\ H^+ \qquad (2)$$

$$CH_3CH_2OH + H_2O \rightarrow CH_3CO_2H + 4\ e^- + 4\ H^+ \qquad (3)$$

$$CH_3CH_2OH + 3 H_2O \rightarrow 2 CO_2 + 12 e^- + 12 H^+ \qquad (4)$$

The stoichiometry of the ethanol oxidation reaction (n_{av}) is also a central parameter in the electrolysis of ethanol, since it determines the ratio of hydrogen production to the consumption of ethanol. Determination of n_{av} in a DEFC is very difficult because of the crossover of ethanol to the cathode where it reacts chemically with oxygen [9]. However it can be determined accurately in an EEC, where ethanol is only consumed electrochemically [9, 10]. Therefore, in this work, n_{av} has been determined in an EEC, by measurement of the amount of ethanol consumed (eq. 5) [9],

$$n_{av} = i/uF(C_{in} - C_{out}) \qquad (5)$$

where i is the average current, u is the flow rate of the ethanol solution, C_{in} is the initial ethanol concentration, and C_{out} is the concentration of ethanol in the combined anode and cathode exhausts.

The multiplication of the potential and faradaic efficiency terms in eq. 1 means that both must be high to provide a competitive overall efficiency. However, this has not yet been achieved [1]. For proton exchange membrane cells, Pt anode catalysts can provide relatively high faradaic efficiencies [9, 11], but potential efficiencies are low. Alloying of Pt with Ru and/or Sn (for example) can significantly increase the potential efficiency [12], but results in lower faradaic efficiencies [13-15]. The purpose of the work reported here was therefore to explore the effects of combining discrete Pt and PtRu catalysts as a mixture or in separate layers in the anode of an EEC. It was postulated that the acetaldehyde intermediate formed at the PtRu catalyst could be oxidized at the Pt catalyst to increase the faradaic efficiency, while maintaining the higher potential efficiency of the PtRu catalyst.

2. EXPERIMENTAL

A commercial fuel cell (5 cm^2 active area; Fuel Cell Technology Inc.) with small modifications [10] was used with a 4 mg cm^{-2} Pt black cathode, Nafion^{TM} 115 membrane (acidic polymer electrolyte) and various anodes. The gaskets were 0.25 mm fibre-glass reinforced Teflon on each side of the membrane. The compression was ca. 15 kg cm^{-2} [16]. Ethanol (Commercial Alcohols Inc.) solution (0.100 M in water) was supplied to the anode at 0.2 or 0.5 mL min^{-1} with a syringe pump and N$_2$ was passed over the cathode at 35 mL min^{-1} to avoid interference from oxygen. The cathode acts a dynamic hydrogen anode (DHE). Electrochemical measurements were made at 80 ºC under steady state conditions and constant cell potentials using a Hokuto Denko HA-301 potentiostat.

Anodes were prepared using commercial carbon supported Pt (HiSPEC® 13100, 70% Pt on a high surface area advanced carbon support (Alfa Aesar; Lot# M22A026)) and PtRu alloy (HiSPEC® 12100, 50% Pt and 25% Ru on a high surface area advanced carbon support (Alfa Aesar; Lot# P17B047)) catalysts. Suspensions of the catalyst in a ca. 1:1 mixture of 1-propanol and Nafion® solution (Dupont; 5% Nafion) were spread onto Toray^{TM} carbon fiber paper (CFP; TGP-H-090; 0.23 mm) with a spatula to give a metal loading of 3.2 mg cm^{-2}. For preparation of the bilayer anodes, a 1.6 mg cm^{-2} Pt layer was applied to the CFP, allowed to dry, and then coated with a 1.6 mg cm^{-2} PtRu layer (designated as Pt on PtRu relative to the membrane; see Fig. 2A), or *vice versa* (PtRu on Pt). Electrodes were allowed to dry overnight at ambient temperature to remove residual propanol. Smooth, uniform catalyst layers with a thickness of ca. 40 µm were obtained.

Each membrane and electrode assembly was broken in over a period of days. The cell was flooded with water for one day at room temperature to hydrate the membrane and then flushed with water at 80 °C for 1 h. It was then operated at 0.7 V for at least 2 h before recording

polarization curves from 0.7 V to 0.1 V and from 0.1 V to 0.7 V (0.05 V steps for 300 s). There was only minor hysteresis between the two curves. Preliminary CO_2 measurements were made and then the cell was shut-down and flushed with water. The reported measurements were made after one of more days of stable operation, from 0.7 to 0.1 V following operation at 0.7 V for at 1 h.

For analysis of the reaction products and residual ethanol, the anode and cathode exhausts were combined in a trap cooled with a mixture of ice and dry ice. CO_2 remaining in the N_2 stream was measured in real time with a commercial non-dispersive infrared CO_2 monitor (Telaire 7001) [15]. The current and CO_2 readings were allowed to stabilize, and then averaged over a period of at least 100 s. The liquid collected in the trap was analyzed by ^{1}H-NMR as previously described [10]. The measured concentrations of ethanol, acetic acid, acetaldehyde and CO_2 were used to determine the faradaic yield of each product. The average charge balance was 98.4±2.2% and the average mass balance was 99.4±1.4%, indicating that the product collection efficiency was high and that no other products (such as CH_4 which would have been lost into the gas stream) were formed in significant quantities. Other possible minor products [9] would have been seen in the NMR spectra if produced in significant quantities.

3. RESULTS AND DISCUSSION

3.1 Polarization curves

Fig. 1 shows polarization curves for the oxidation of 0.100 M ethanol at anodes prepared with the Pt and PtRu catalysts individually, with a homogeneous mixture of the two catalysts, and with discrete layers of the catalysts. The data for the individual catalysts has been previously presented and discussed [9]. The PtRu catalyst oxidizes ethanol at a lower potential than Pt because Ru-OH is formed at lower potentials than Pt-OH. However, the main product is acetic acid rather than CO_2. Pt, which oxidizes as much as 50% of the ethanol to CO_2 [9], provides

higher currents than PtRu at potentials above ca. 0.45 V because of the higher number of electrons transferred per molecule of ethanol. Based on this analysis of the differences between Pt and PtRu, the mixed Pt + PtRu layer would be expected to provide higher currents than Pt alone at low potentials, but lower currents at high potentials, and that is what is observed in Fig. 1. However, there was a narrow region at ca. 0.45 V where the mixed layer gave higher currents than either catalyst alone, indicating that there was a synergy between the two catalysts.
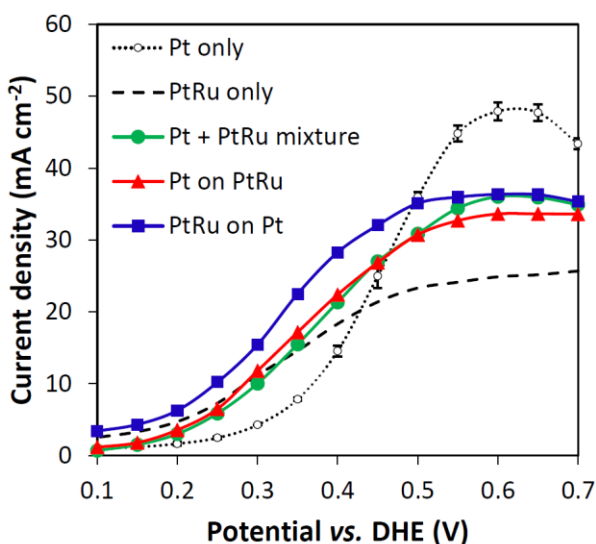

Figure 1. Polarization curves for the oxidation of 0.100 M ethanol (0.5 mL min^{-1}) at Pt (·····), PtRu (- - -), Pt + PtRu (●), Pt on PtRu (▲) and PtRu on Pt (■) anodes at 80 ºC. Averages and standard deviations are shown for two different Pt anodes.

Since PtRu provides the fastest oxidation of ethanol at low potentials, and produces significant amounts of acetaldehyde at low potentials [9], it was envisaged that a Pt layer on top of a PtRu layer could be used to oxidize the acetaldehyde before it left the catalyst layer, and thereby increase the overall efficiency of ethanol oxidation. This is shown schematically in Fig. 2A. Because of the low activity of the Pt catalyst at low potentials, most of the ethanol will diffuse through the Pt layer to the PtRu layer, although some will be oxidized in the Pt layer (not shown in Fig. 2A). However, the polarization curve for the Pt on PtRu bilayer in Fig. 1 is not

consistent with this scenario because the currents observed at potentials below 0.3 V were lower than at the PtRu anode, and the polarization curve was not significantly different from that for the mixture of Pt with PtRu. Curiously, reversing the order of the two catalyst layers produced higher currents than all of the other anodes for potentials below 0.5 V, although Pt produced higher currents at higher potentials.
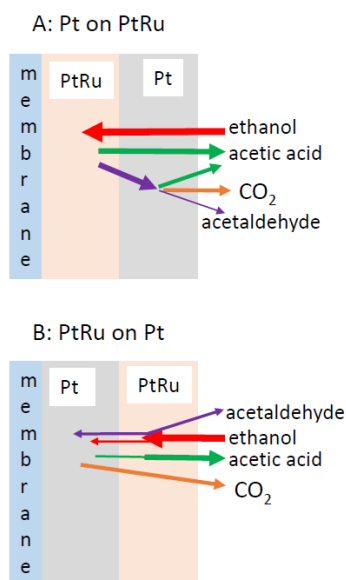

Figure 2. Schematic diagrams of some of the reactions and transport processes within bilayer anodes. Arrow widths represent approximate linear diffusion fluxes of ethanol (red), acetaldehdye (purple), acetic acid (green) and CO_2 (orange) into, within, and out of the catalyst layer. Non-horizontal line are used for clarity and labelling only.

Overall, the mixed anode and both bilayers showed significant synergy between the Pt and PtRu catalysts. In order to understand this, and the differences seen in the polarization curves for the various anodes containing both Pt and PtRu, product distributions were measured as a function of potential. These, combined with the currents, allow the net rate of formation of each product to be obtained, which provides insight into the synergies between the two catalysts.

3.2 Product distributions

Figure 3A shows faradaic yields of CO_2, acetic acid, and acetaldehyde obtained from analysis of the products in the cell exhaust. Two different Pt anodes were tested in order to check an anomalous dip in the CO_2 yield seen at ca. 0.4 V. Full product analysis for the second Pt anode focused on the 0.3 to 0.45 V region and so the data for the two Pt anodes is plotted separately. It has been speculated that the two peaks seen in the CO_2 yield at Pt may be due to a change in mechanism [9].

The yields of CO_2 obtained for the bilayers and mixed Pt + PtRu layer were intermediate between those for Pt and PtRu alone, with the exception of the PtRu on Pt bilayer at 0.4 V which gave a slightly higher yield than Pt alone. At 0.2 and 0.3 V, the CO_2 yields for the bilayer and mixed anodes were closer to those for PtRu, but increased sharply at higher potentials to become closer to the values for Pt. This is highly significant because the CO_2 yield is the dominant factor determining the faradaic efficiency, and the high CO_2 yields for the bilayer anodes are obtained at much higher current densities than for Pt. Most notably, at 0.4 V the PtRu on Pt bilayer produced a CO_2 yield of 59% at 28 mA cm^{-2}, while the Pt anode provided 56% CO_2 at 13 mA cm^{-2}.

Acetic acid yields for the mixed and bilayer anodes were also intermediate between those for Pt and PtRu alone (Fig. 3B), and closer to those for PtRu at low potentials and Pt at high potentials. However, acetaldehyde yields were generally lower at the mixed and bilayer anodes than either the Pt or PtRu anodes. For the PtRu on Pt anode, the yield of acetaldehyde was only 56% of the yield for the PtRu anode, on average. This validates the strategy of using Pt to oxidize the acetaldehyde produced by the more active PtRu catalyst before it can leave the anode, illustrated in Fig. 2. Both the mixed and bilayers anodes gave very low yields of acetaldehyde at 0.35 V and higher. The average acetaldehyde yield was only 1.1% for the PtRu on Pt anode over

the potential range of 0.35 to 0.7 V. Neither the order of the two layers nor whether the catalysts were mixed affected the acetaldehyde yield significantly. This, together with the relatively small yields of acetaldehyde at all of the anodes at > 0.4 V (Fig. 3C), indicates that there was some other, more important factor responsible for the high activity and CO_2 to acetic acid ratios for the PtRu on Pt bilayer anode.
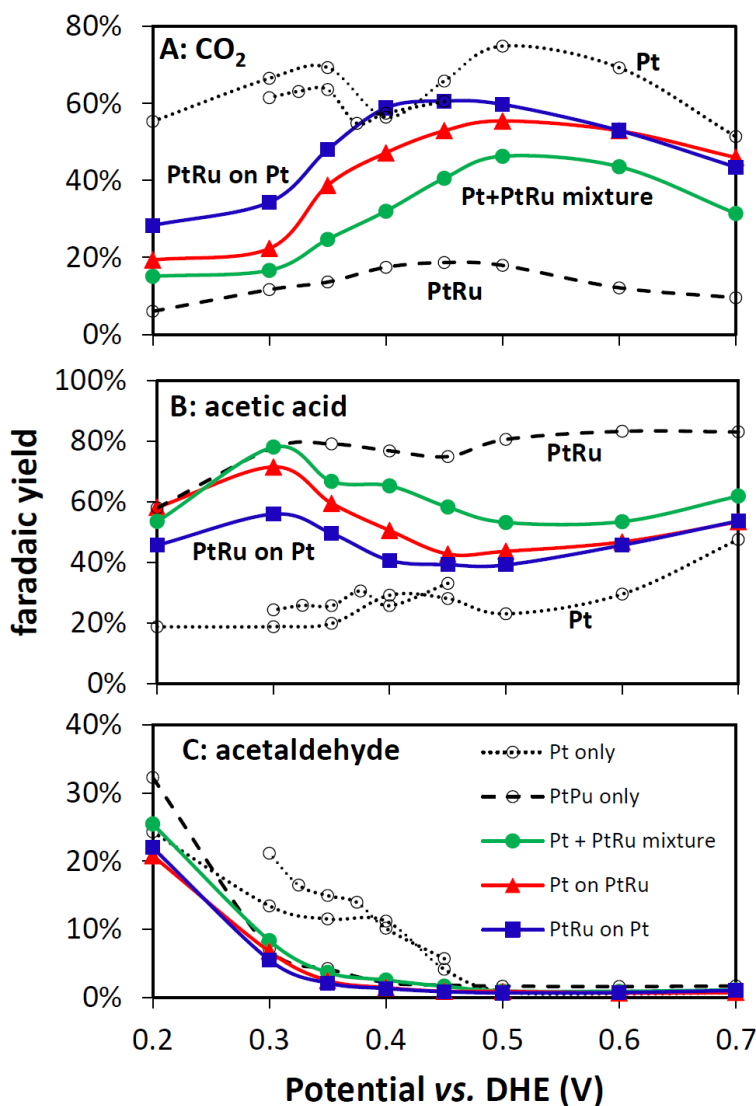

Figure 3. Faradaic yields of CO_2 (A), acetic acid (B), and acetaldehyde (C) *vs.* potential for oxidation of 0.100 M ethanol (0.2 mL min^{-1}) at Pt (·····; data for 2 different anodes), PtRu (- - -), Pt + PtRu (●), Pt on PtRu (▲) and PtRu on Pt (■) anodes at 80 °C.

3.3. Stoichiometry and efficiency

Figure 4 shows n_{av} as a function of potential for the oxidation of ethanol at the Pt, PtRu, mixed and bilayer anodes, obtained from the concentration of ethanol consumed (eq. 5). At most potentials, n_{av} values for the mixed and bilayer anodes were intermediate between those for the Pt and PtRu catalysts alone, as would be expected. However, from 0.35 to 0.45 V n_{av} for the bilayer anodes was close to, and even exceeded, the values for Pt. n_{av} was generally lower for the mixed anode, and at low potentials was close to the values for PtRu alone.
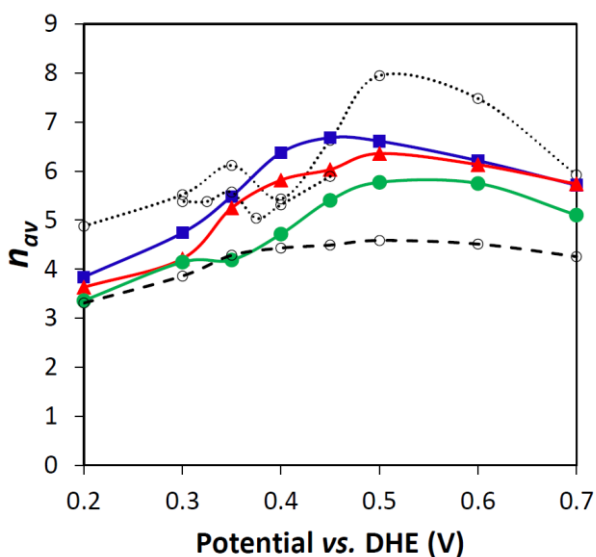

Figure 4. n_{av} from eq. 5 *vs.* potential for the oxidation of 0.100 M ethanol (0.2 mL min^{-1}) at Pt (·····; data for 2 different anodes), PtRu (- - -), Pt + PtRu (●), Pt on PtRu (▲) and PtRu on Pt (■) anodes at 80 ℃.

The high n_{av} at 0.40 V for the bilayers, relative to Pt or PtRu alone, leads to significant increases in fuel efficiency for ethanol electrolysis, and the higher current densities would decrease system costs. Use of the bilayers would also increase the thermal efficiency ($\varepsilon_{rev}\varepsilon_E$) and overall efficiency of a DEFC, because the cell potential would be higher and less ethanol would be consumed. However, this is difficult to demonstrate and quantify with a DEFC because of the effects of crossover of ethanol to the cathode, where it reacts chemically with oxygen [9, 10, 17].

Consequently, representative DEFC efficiencies were calculated by using eq. 1, with E_{cell} estimated from the anode potentials *vs*. DHE in Fig. 1 and a cathode polarization curve for the same cell [9, 18]. The results are shown in Fig. 5 as functions of the power density (A) and current density (B) of the DEFC. Since the loss of fuel due to crossover will depend on many factors, including the membrane, cell design and operating conditions, it was not included in these efficiency estimates (i.e. $\varepsilon_C = 1$ in eq. 1).
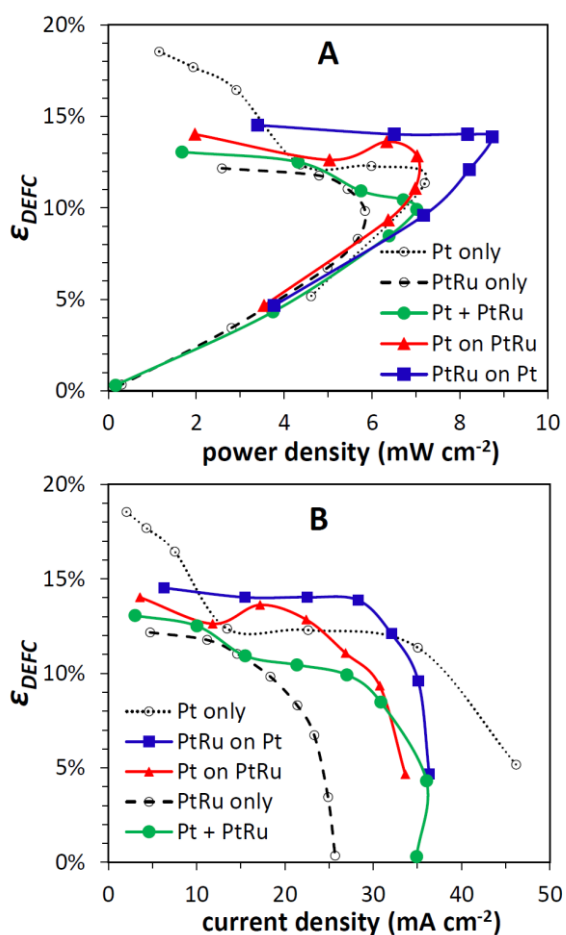

Figure 5. Predicted efficiency vs. power density (A) and current density (B) for DEFCs operating with 0.100 M ethanol at 80 °C at Pt ($\cdots$), PtRu (- - -), Pt + PtRu (●), Pt on PtRu (▲) and PtRu on Pt (■) anodes.

Surprisingly, the Pt catalyst would provide the best efficiency at the lowest power and current densities. Although the PtRu and PtRu on Pt anodes gave much higher currents at low

potentials, which provide the highest potential efficiencies, this is more than offset by the lower stoichiometry (e.g. $n_{av} = 6.1$ for Pt at 7.5 mA cm^{-2} *vs.* $n_{av} = 3.8$ for PtRu on Pt at 6.3 mA cm^{-2}). At higher power densities (ca. 4-9 mW cm^{-2}), the PtRu on Pt anode would provide significantly higher efficiencies than Pt due to the lower anode potential, since the stoichiometries were similar. The Pt on PtRu anode would also be more efficient than Pt at ca. 5-7 mW cm^{-2}. Neither the PtRu anode nor the mixed Pt + PtRu anode would provide better efficiency or maximum power density than the Pt anode. These differences between the efficiencies of the anodes are paralleled in the plots of efficiency *vs.* current density.

3.4. Reaction rates

The polarization curves shown in Fig. 1 are somewhat misleading because the currents are determined by the rates of three simultaneous reactions (equations 2-4). Since the relative rates of these reactions vary with potential, the current does not provides an accurate reflection of the rate at which ethanol is oxidized (consumed). However, this can be extracted from the data by using eq. 6

$$\text{rate of ethanol oxidation (mol s}^{-1}) = i/n_{av}F \qquad (6)$$

Figure 6 shows the calculated ethanol oxidation rates as a function potential, based on n_{av} values obtained from eq. 5, and the average currents measured during collection of the samples for NMR analysis. The rate of ethanol consumption at the Pt anode was initially very low because of the low currents and high CO_2 yields, but increased sharply at potentials above 0.35 V as the current increased. Ethanol consumption at low potentials was much faster at the other anodes, and began to level off at high potentials as the currents plateaued. Curiously, the ethanol consumption rates were similar for the mixed, bilayer, and PtRu anodes, and increased approximately linearly with potential up to ca. 0.4 V. Thus, although the current increased

exponentially with potential (Tafel behavior), indicating control by an electron transfer rate, the rate of ethanol consumption does not appear to have been limited by an electron transfer step.
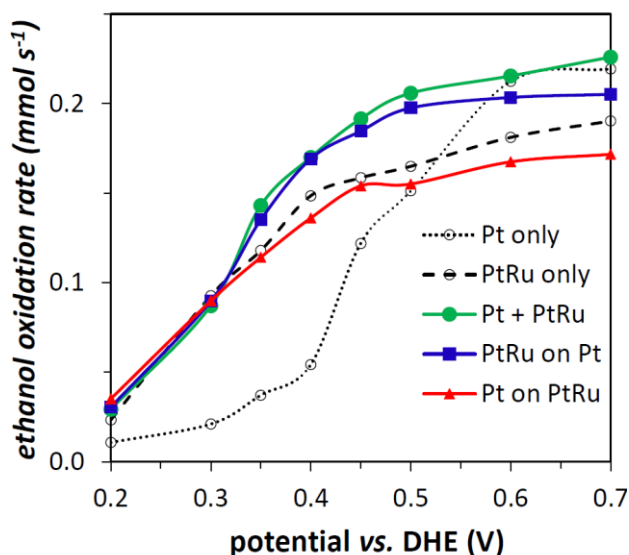

Figure 6. Ethanol consumption rate *vs.* potential for the oxidation of 0.100 M ethanol (0.2 mL min^{-1} and 80 $^\circ$C) at Pt ($\cdots$), PtRu (- - -), Pt + PtRu ($\bullet$), Pt on PtRu ($\blacktriangle$) and PtRu on Pt ($\blacksquare$) anodes.

Further insight into this behavior can be obtained from the potential dependence of the rate of formation of each product, shown in Fig. 7. The rates of CO_2 formation increased approximately exponentially with potential between 0.2 and 0.4 V, as expected for a process limited by the rate of an electron transfer. It leveled off at higher potentials, presumably due to the effects of concentration polarization (mass transport limitation). The mixed and bilayer anodes produced CO_2 at similar rates to the Pt anode, while the rate was significantly lower at PtRu. It can therefore be concluded that CO_2 was produced primarily by the Pt catalyst in the mixed and bilayer anodes. The higher rate of CO_2 production at the PtRu on Pt anode relative to the Pt on PtRu anode or mixed anode appears to be inconsistent with this, since less ethanol would reach the Pt layer because of consumption in the PtRu layer, as illustrated in Fig. 2B. However, this apparent anomaly can be explained by the increase in CO_2 yield that occurs at Pt

anodes as the ethanol concentration is decreased [11, 19, 20]. This is supported by, and explains, the higher CO_2 yields obtained with the PtRu on Pt anode (Fig. 3).
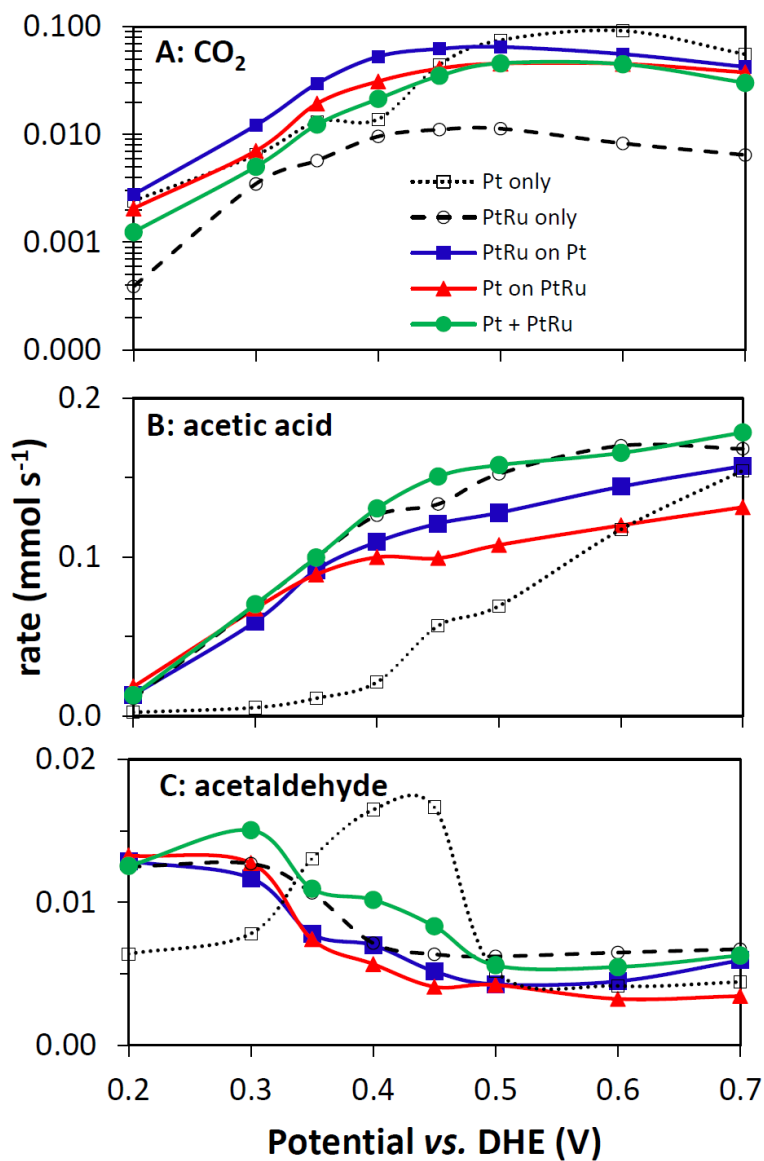

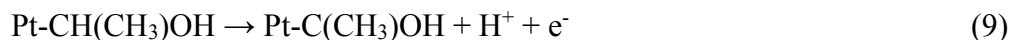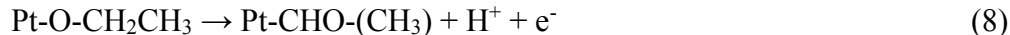**Figure 7.** Product production rates *vs.* potential for the oxidation of 0.100 M ethanol (0.2 mL min^{-1} and 80 $^\circ$C) at Pt ($\cdots$), PtRu (- - -), Pt + PtRu ($\bullet$), Pt on PtRu ($\blacktriangle$) and PtRu on Pt ($\blacksquare$) anodes.

In contrast to the normal exponential dependence of the rate of CO_2 formation on potential, the rate of acetic acid formation increased linearly with potential for the PtRu, mixed and bilayer anodes at low potentials. This suggests that the rate of acetic acid formation at these anodes was controlled by a chemical step. The rate of acetaldehyde formation generally decreased with increasing potential, except for the Pt anode which gave a pronounced peak at ca. 0.4 V. The complex variations in acetaldehyde production with potential arise because it is simultaneously produced and consumed by both catalysts.

At potentials from 0.2 V to 0.35 V, the rate of acetic acid production was very low at the Pt anode, due to the low currents and yields. Over this potential range, the PtRu, mixed and bilayer anodes produced acetic acid at similar rates that were much higher than for Pt. It can therefore be concluded that acetic acid was formed primarily by the PtRu in the mixed and bilayer anodes. The order of the layers did not have a significant effect because only a small amount of ethanol was consumed by the Pt catalyst at low potentials. At higher potentials, the increased consumption of ethanol by the Pt layers caused the rate of acetic acid formation to drop below the rate for the PtRu anode.

3.5. Mechanisms

Although the simple model illustrated in Fig. 2 provides significant insight into the performances and product distributions obtained from the bilayer anodes, it does not explain why both bilayers provided better performances than a mixture of the Pt and PtRu catalysts, and much better performances than PtRu alone. Further insight can be obtained by considering mechanistic information and models that have been reported in the literature. It is generally accepted that the initial stages of ethanol oxidation at Pt based anodes proceed through two successive electrochemical dehydrogenation steps (eqs. 7-9) that lead to the formation of adsorbed acetaldehyde (eq. 8) and an adsorbed CH_3COH species (eg. 9) [21, 22].

$$CH_3CH_2OH \rightarrow (Pt\text{-}O\text{-}CH_2CH_3 \text{ or } Pt\text{-}CH(CH_3)OH) + H^+ + e^- \qquad (7)$$

$$Pt\text{-}O\text{-}CH_2CH_3 \rightarrow Pt\text{-}CHO\text{-}(CH_3) + H^+ + e^- \qquad (8)$$

$$Pt\text{-}CH(CH_3)OH \rightarrow Pt\text{-}C(CH_3)OH + H^+ + e^- \qquad (9)$$

$Pt\text{-}C(CH_3)OH$ (i.e. CH_3COH_{ad}) is thought to be the precursor to the formation of acetic acid and CO_2 [23], while acetaldehyde is produced by desorption following reaction 8, or through the reaction of adsorbed ethanol with a surface hydroxyl group [24].

In contrast to the dehydrogenation of ethanol to adsorbed C_2 species, the C-C of acetaldehyde is broken during adsorption [22]. Consequently, acetaldehyde generates adsorbed C_1 species at lower potentials than ethanol [22, 25]. Cleavage of the C-C bond to form CO_{ad} and $CH_{x,ad}$ is thought to be a chemical step [26].

These mechanistic differences between acetaldehyde and ethanol oxidation presumably play a significant role in the synergy observed here between layers of Pt and PtRu catalysts. In the low potential region between 0.2 and 0.4 V where the synergy is strongest, most of the ethanol is oxidized by the PtRu catalyst to produce acetaldehyde and acetic acid. For the Pt on PtRu anode, some of the acetaldehyde crosses the membrane to the cathode [10], but most diffuses into the Pt layer, where it can adsorb and dissociate to CO_{ad} and $CH_{x,ad}$. At the 80 °C operating temperature of the cell, these C_1 species are oxidized almost exclusively to CO_2 at Pt. This is indicated the excellent mass balances obtained for ethanol oxidation at all anodes, since significant formation of other, undetected C_1 products, such as CH_4, would lead to low mass balances. The high yields of CO_2 observed at 0.2 to 0.35 V for the Pt anode in Fig. 3 demonstrate that Pt can efficiently oxidize the acetaldehyde intermediate to CO_2 under the conditions employed here, since ethanol is dehydrogenated to acetaldehyde prior to breaking of the C-C bond at low potentials [22]. This is also supported by the >75% yield of CO_2 that has been reported for the oxidation of acetaldehyde at a carbon supported Pt anode at 80 °C [27].

It was envisaged that the Pt on PtRu bilayer configuration (Fig. 2A) would be superior to the PtRu on Pt configuration (Fig. 2B) because more of the acetaldehyde produced in the PtRu layer would pass into the Pt layer. However, this effect appears to have been outweighed by the effect the PtRu layer on the concentration of ethanol in the Pt layer. Rationalization of the performance of the mixed anode relative to the bilayer anodes is more difficult. Having Pt nanoparticles close to all of the PtRu nanoparticles should be beneficial for oxidation of acetaldehyde, but this is not supported by the yields of acetaldehyde which were similar to (94% of, on average) those for PtRu alone. The effect of ethanol concentration for the mixed anode should have been intermediate between the effects for the two bilayer configuration, but the low CO_2 yields show that this was not the case. The main synergistic effect in the mixed electrode, seen at 0.4 V in the polarization curve (Fig. 1), correlates with the anomaly in the product distribution at 0.4 V for Pt alone (Fig. 3). The addition of PtRu eliminates the peak in acetaldehyde production seen for Pt alone in this region (Fig. 3C), possibly by decreasing the local ethanol concentration.

4. CONCLUSIONS

The goals of combining Pt and PtRu catalysts to increase the low potential performance of anodes for ethanol oxidation, and decreasing acetaldehyde production, have been achieved. There is a synergy between the Pt and PtRu catalysts in both the mixed anode and bilayer structures that appears to be due to the oxidation at the Pt catalyst of acetaldehyde produced at the PtRu catalyst. The PtRu on Pt bilayer structure provides the added benefit that the PtRu layer decreases the ethanol concentration before it reaches the Pt layer, which leads to higher CO_2 yields. Since all of the anodes employed in this work had the same total metal loading (3.2 mg cm^{-2}), the bilayer anodes contained less Pt than the Pt anode and so would lower the cost in addition to increasing performance and efficiency.

The importance of determining the stoichiometry of ethanol oxidation, and the product distribution, is demonstrated by the efficiencies presented in Fig. 5 and the product production rates presented in Fig. 7. Even with the strong synergy between the Pt and PtRu catalysts observed for the PtRu on Pt anode, the Pt catalyst alone produced the highest overall efficiency (18.5%). This highlights the need for further improvement of CO_2 yields at low potentials. The data in Fig. 7 show that Tafel analysis of the total current will produce ambiguous results, since a large component of the current is not limited by electron transfer kinetics. Accurate analysis of the kinetics of ethanol oxidation will require fitting of the rates of each reaction to a detailed mechanistic model.

ACKNOWLEDGEMENTS

REFERENCES

[1] L. An, T.S. Zhao, Y.S. Li, Renew. Sustain. Energy Rev., 50 (2015) 1462-1468.

[2] S.P.S. Badwal, S. Giddey, A. Kulkarni, J. Goel, S. Basu, Applied Energy, 145 (2015) 80-103.

[3] S. Ramachandran, U. Stimming, Energy Environ. Sci., 8 (2015) 3313-3324.

[4] H.R. Corti, E.R. Gonzalez, in: Direct Alcohol Fuel Cells, Springer, Dordrecht 2014.

[5] V. Bambagioni, M. Bevilacqua, C. Bianchini, J. Filippi, A. Lavacchi, A. Marchionni, F. Vizza, P.K. Shen, ChemSusChem, 3 (2010) 851-855.

[6] D. Banham, S.Y. Ye, ACS Energy Letters, 2 (2017) 629-638.

[7] O.Z. Sharaf, M.F. Orhan, Renew. Sustain. Energy Rev., 32 (2014) 810-853.

[8] U.B. Demirci, J. Power Sources, 169 (2007) 239-246.

[9] R.M. Altarawneh, P.G. Pickup, J. Electrochem. Soc., 164 (2017) F861-F865.

[10] R.M. Altarawneh, P. Majidi, P.G. Pickup, J. Power Sources, 351 (2017) 106-114.

[11] S. Sun, M.C. Halseid, M. Heinen, Z. Jusys, R.J. Behm, J. Power Sources, 190 (2009) 2-13.

[12] E. Antolini, J. Power Sources, 170 (2007) 1-12.

[13] S. Rousseau, C. Coutanceau, C. Lamy, J.M. Leger, J. Power Sources, 158 (2006) 18-24.

[14] N. Nakagawa, Y. Kaneda, M. Wagatsuma, T. Tsujiguchi, J. Power Sources, 199 (2012) 103-109.

[15] A. Ghumman, G. Li, D.V. Bennett, P. Pickup, J. Power Sources, 194 (2009) 286-290.

[16] C. Song, P.G. Pickup, J. Appl. Electrochem, 34 (2004) 1065-1070.

[17] D.D. James, P.G. Pickup, Electrochim. Acta, 55 (2010) 3824-3829.

[18] G. Li, P.G. Pickup, J. Power Sources, 161 (2006) 256-263.

[19] D.D. James, P.G. Pickup, Electrochim. Acta, 78 (2012) 274-278.

[20] P. Majidi, P.G. Pickup, Electrochim. Acta, 182 (2015) 856–860.

[21] J. Florez-Montano, G. Garcia, O. Guillen-Villafuerte, J.L. Rodriguez, G.A. Planes, E. Pastor, Electrochim. Acta, 209 (2016) 121-131.

[22] J. Torrero, F.J. Perez-Alonso, M.A. Pena, C. Dominguez, A.O. Al-Youbi, S.A. Al-Thabaiti, S.N. Basahel, A.A. Alshehri, S. Rojas, Chemelectrochem, 3 (2016) 1072-1083.

[23] R. Kavanagh, X.M. Cao, W.F. Lin, C. Hardacre, P. Hu, Angew. Chem. Int. Ed. Engl., 51 (2012) 1572-1575.

[24] R. Kavanagh, X.M. Cao, W.F. Lin, C. Hardacre, P. Hu, Journal of Physical Chemistry C, 116 (2012) 7185-7188.

[25] M. Heinen, Z. Jusys, R.J. Behm, J. Phys. Chem. C, 114 (2010) 9850–9864.

[26] A.B. Delpeuch, C. Cremers, M. Chatenet, Electrochim. Acta, 188 (2016) 551-559.

[27] S. Sun, M. Heinen, Z. Jusys, R.J. Behm, J. Power Sources, 204 (2012) 1-13.